Modeling acoustic channel variability in underwater network simulators from real field experimental data

Nicola Toffolo‡, Antonio Montanari‡, Filippo Campagnaro‡, Michele Zorzi‡

‡ Department of Information Engineering, University of Padova, via Gradenigo 6/B, 35131 Padova, Italy,
‡{toffolonic,montanar,campagn1,zorzi}@dei.unipd.it

Abstract—**The features of the underwater acoustic channel are remarkably dependent on the considered scenario; for instance, the link quality differs significantly in shallow water with respect to deep water, and series of events such as the presence of rain or ships passing nearby, changes of temperature and wind strength, can change drastically the channel conditions observed in a certain area in different seasons and even during the same day. Mathematical models that consider these parameters exist, but are either very computationally demanding, like the Bellhop ray tracer, or not sufficiently accurate, like the Urick model that often exhibits optimistic results. In this paper, we discuss the development of a statistical channel model based on the analysis of real field experimental data and compare its performance with the other channel models available in the DESERT Underwater network simulator.**

Index Terms—**Underwater networks, underwater acoustic channel, Hidden Markov Model.**

I. INTRODUCTION AND RELATED WORKS

Underwater acoustic networks (UANs) are widely used in both military and civilian applications, including, but not limited to, coastal surveillance and monitoring, tsunami prevention and oil and gas pipeline inspection. While sea trials are the best way to evaluate UANs, their realization is highly demanding in terms of costs, time, personnel and equipment. For this reason, network simulators are often employed for a preliminary evaluation, in order to debug the protocol stack before the final sea trial. However, simulations are still not considered to be a valuable tool to perform the final evaluation of UANs, as channel models can hardly describe the time-varying behavior of a real acoustic channel [1]. Long-term variability is dominant in underwater acoustic links, which are characterized by high Packet Error Rate (PER) and Round Trip Time (RTT) values; they may be robust to multipath effects but struggle when the signal to noise ratio (SNR) decreases [2]. This implies that relying on a classical Gaussian or Rician distribution to understand channel performance will not lead to accurate results, unless we are considering simpler short-term dependencies [3]. A number of factors are responsible for this behavior: from temperature, wind, water currents, to Doppler caused by Vortex Induced Vibrations (VIV) [4] or bubbles brought by tidal inflow and produced by ship propellers in a near shipping lane [5]. Furthermore, the use of realistic channel models, such as the Bellhop ray tracer [6], is highly

computationally demanding and hence restricted to networks with a small number of nodes. Given that a number of sea experiments have been performed by scientists in the last 15 years [7]–[11], a wide dataset of time evolution of the link quality has been collected, and some measurements are publicly available. Data-driven models have thus been used to predict the trend of channel performance; for example, in [12] the authors, considering different environmental characteristics as features for the model, build a logistic regression network whose Packet Success Rate estimates are quite fair if restricted to a short-term variability of an acoustic link. In [7] the authors present the ASUNA dataset, a collection of the time evolution of acoustic links in six different sea and lake trials: during each trial an underwater network was tested with different topologies. They also show how the time varying links can be used in a Matlab network simulation in order to reproduce the link quality evolution experienced during those sea trials. Similarly, in [13] the authors included in the DESERT Underwater network simulator [14] the time evolution of the links of the multimodal acoustic mobile ad hoc network deployed in [10] and composed of low frequency and high frequency modems. Both solutions can certainly reproduce the time evolution of these experiments, but their main drawback is that they do not allow to test different channel realizations.

According to [15], [16], the time evolution of underwater acoustic channels can be statistically well characterized with two- and four-state Markov models and with a two-state Hidden Markov Model (HMM) [17]. While in terrestrial networks the transition probabilities from the states of the Markov Chain used to model the channel are usually obtained using well-established statistical channel characterizations such as Rayleigh fading or Rician fading channel models [18], in underwater acoustic networks there is no commonly accepted statistical model for the channel behavior, hence the parameters of the Markov model are inferred from experimental measurements. The authors in [16] showed that the HMM yields an accurate reproduction of the channel metrics, tracking well long term channel behaviors, and making it a good choice for modeling the channel in UANs simulators.

This work presents a statistical model based on the analysis of sea trial data, and compares the accuracy of this model with respect to already existing models. This model is included in the DESERT Underwater framework [14], that counts a wide set of protocols for best customizing the underwater network.

The model's parameters are inferred from measurements coming from the ASUNA dataset [19], which includes time series of link quality indicators, measured during the aforementioned experiments.

The paper is organized as follows. Section II presents the dataset used to configure the channel model parameters; Section III describes the details of the statistical model and its implementation in the simulator; Section IV evaluates the performance of our model when compared to legacy mathematical models, and shows the results of the simulations and, finally, Section V concludes the paper.

II. DATASET DETAILS

The data used to train the statistical model presented in this paper was extracted from the ASUNA dataset. Specifically, we used the data of the Haifa harbor (Israel) test performed in May 2009 [20]. 4-meter rubber boats were used to deploy the nodes in six distinct topologies. In this paper we analyzed the behavior of the model trained with the data of topology 1 (Figure 1a) and topology 2 (Figure 1b). Actually, topologies 1 and 2 do not have any physical difference as the nodes were kept in the same position. Still, the changes on channel quality resulted in a difference of the logical topology, as the link between nodes 1 and 3 was disrupted. A spatial reuse TDMA protocol (each device had a dedicated 5-second slot for transmission) was tested, and the transmission rate of the modems was 600 bps without channel coding.
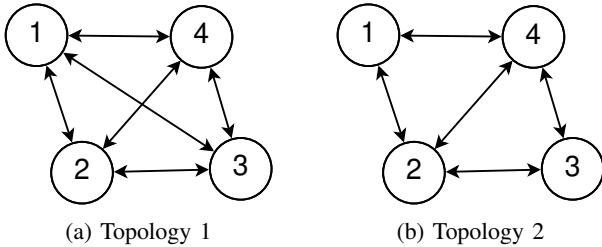

(a) Topology 1   (b) Topology 2

Fig. 1: Topologies analyzed in this paper.

The link quality indicator observed during the trial is the Bit Error Rate (BER), defined as the ratio between the number of erroneous bits and the number of transmitted bits. The dataset provides a set of time-varying BER per-link values collected into 3D `TxNxN` matrixes (one per topology), where T is the number of time slots, N is the number of nodes in the network, and the entry (t, i, j) represents the BER value for the link from node i (transmitter) to node j (receiver) in time slot t. The time slot lasts 1 s, and at each measurement BER and GPS position (in UTM coordinates) of each node are recorded. During the sea trial, Topology 1 was tested for 30 minutes, while Topology 2 was tested for 60 minutes.

A. Time Variability of BER

During the experiment the BER of each link was varied in time. In some of the links almost no errors were experienced for almost all the time, while other links had a higher error rate.
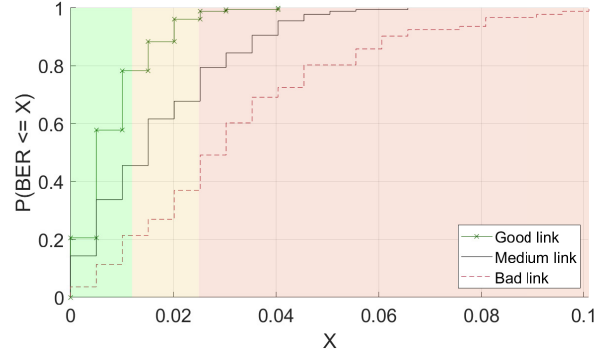

Fig. 2: Examples of CDF for a stable link (green line with cross markers), an average link (black line), and a challenging link (dashed red line).

For instance, in Figure 2 we can observe the BER Cumulative distribution function (CDF) of three representative links observed during the trial.

Specifically, the green line with cross markers refers to the CDF of the very stable link from node 4 to node 2 observed in topology 2, whose BER is lower than 0.02 for 90% of the time. The black line, instead, refers to the CDF of the link from node 3 to node 2 observed in topology 2: in this case the BER is slightly higher than the previous case but never exceeds 0.06. Finally, the red dashed line is associated to the link from node 1 to node 3 observed in topology 1: this link has a BER that is definitely higher than the other two links.

III. CHANNEL MODEL

In this section we present a two-state (Figure 3a) and a three-state (Figure 3b) HMMs trained with the ASUNA dataset and used to simulate the acoustic channel. Specifically, for each model, we infer from the data i) the packet error probability when the channel is in a certain state, and ii) the transition probability from one state to another. For the two-state HMM we defined only "good" and "bad" states, in order to distinguish between time intervals when the packet reception probability is high and time intervals when the packet error probability is low. For the three-state HMM, instead, we added a state called "medium," to identify when the error rate is lower than in the "bad" state, but still not that low to be considered a good channel.

To analyze the link quality, we first need to define when a link is assumed to be in "good" and "bad" state for the two-state HMM, and in "good," "medium" and "bad" state for the three-state HMM, by observing the Packet Error Rate (PER). To compute the PER, we considered a Hamming(7,4) Forward Error Correction (FEC) and a packet size of 16 bytes without FEC (i.e., 28 bytes with FEC): with this assumption the PER can be computed analytically as:

$$PER = 1 - ((1 - BER)^7 + 7 \cdot BER(1 - BER)^6)^{224/7}. \quad (1)$$

In Tables I and II we report the BER and PER threshold for the two- and the three-state HMMs, respectively. From these
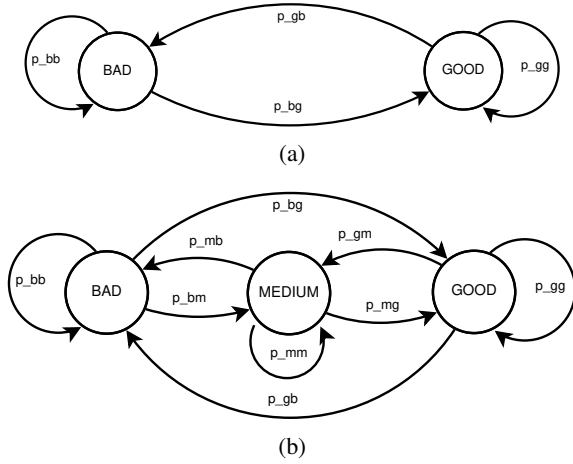
Fig. 3: Two- (a) and three- (b) state channel models.

values we can observe that the "good" channel is the same for both models, while the "bad" channel of the two-state HMM is modeled as two separate states in the three-state HMM.

TABLE I: BER/PER Thresholds Two-State HMM

state	BER	PER
Good	< 0.012	< 0.09
Bad	> 0.012	> 0.09

TABLE II: BER/PER Thresholds Three-State HMM

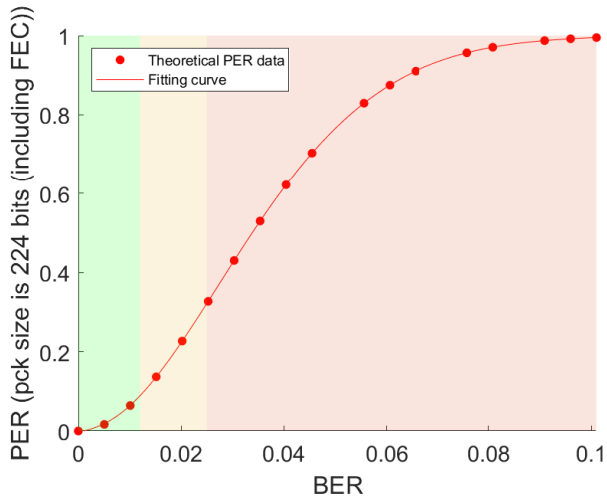| state	BER	PER
Good	< 0.012	< 0.09
Medium	$0.012 < BER < 0.025$	$0.09 < PER < 0.32$
Bad	> 0.025	> 0.32

Fig. 4: PER vs BER values considering a packet with 16-Byte payload and Hamming(7,4) FEC.

We can observe in Figure 4 the PER-BER relation obtained analytically with Eq. (1). Table III shows the averaged BER

values for the two-state HMM of the analyzed links, while Table IV presents the averaged BER for the three-state HMM.

TABLE III: Average BER values, two-state HMM

	avg good	avg bad
Topology 2, link 4→2	0.0051	0.0193
Topology 2, link 3→2	0.0048	0.0267
Topology 1, link 1→3	0.0066	0.0395

TABLE IV: Average BER values, three-state HMM

	avg good	avg medium	avg bad
Topology 2, link 4→2	0.0051	0.0174	0.0281
Topology 2, link 3→2	0.0048	0.0165	0.0338
Topology 1, link 1→3	0.0066	0.0184	0.0448

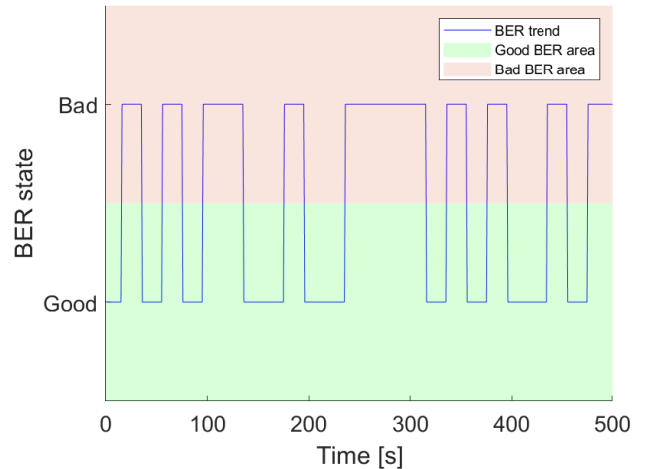With these thresholds, we can compute the generic probability that a link is in one of the states.

Fig. 5: First 500 seconds of the BER time evolution of the link from node 3 to node 2 in topology 2 according to the two-state HMM.

We report an example of the typical BER time evolution of a link in Figure 5, where only two possible states are considered. We can observe that a link in a state i is more likely to remain in that state in the successive time slot (that lasts 1 second), rather than jump to another state. For instance, during the first 100 s the state changes only 5 times in 100 time slots, while in the time interval between 200 and 300 seconds it changes only one time. With this observation, we decided to model the PER time evolution of a generic link as a Markov chain (Figure 3). As already mentioned in this section, we propose a two-state Markov chain with $S_2 = \{G, B\}$ that stand for "Good" and "Bad", and a three-state Markov chain with the three states $S_3 = \{G, M, B\}$ that stand for "Good," "Medium," and "Bad," respectively. Specifically, if we denote as $X_0, \ldots, X_n, \ldots X_N$ a sequence of random variables where X_i takes values in the set S_x, with $x = 2$ for the two-state and $x = 3$ for the three-state Markov chain, the probability $\mathbb{P}(X_{n+1} = j | X_n = i)$ is the *transition probability* from state

i to state j at step n. Additionally, by the Markov property, we have that:

$$\mathbb{P}(X_{n+1} = i_{n+1}|X_0 = i_0, \ldots, X_n = i_n) = \\ \mathbb{P}(X_{n+1} = i_{n+1}|X_n = i_n), \quad (2)$$

which can be interpreted as the fact that, if the current state $X_n = i_n$ is known, the probability of $\mathbb{P}(X_{n+1} = i_{n+1})$ does not depend on the previous states. If the transition probabilities do not depend on n but only on i and j, the Markov chain is *homogeneous* and we may compute every joint probability knowing only the initial distribution of the states $p_i^{(0)} = \mathbb{P}(X_0 = i)$ and the values of p_{ij}, where:

$$p_{ij} = \mathbb{P}(X_{n+1} = j|X_n = i). \quad (3)$$

Exploiting matrix calculus, since we knew the frequencies of the BER values of each link, we found the *transition matrices* $P = (p_{ij})$, which have only non negative elements, and are row-normalized to 1.

A relevant result is that, given the transition matrix at time t, it is possible to compute the n-step transition probabilities by means of matrix exponentiation:

$$\mathbb{P}(X_{t+n} = j|X_t = i) = (P^n)_{ij}, \forall t \geq 0. \quad (4)$$

While with the three-state HMM the transition matrix P^n at step n needs to be computed with matrix exponentiation as presented in Eq. (4), in the simple two-state model the transition probabilities at step n can be obtained via the closed formula [21]:

$$P^n = \frac{1}{p_{gb'} + p_{b'g}} \begin{pmatrix} p_{b'g} & p_{gb'} \\ p_{b'g} & p_{gb'} \end{pmatrix} \\ + \frac{(1 - p_{gb'} - p_{b'g})^n}{p_{gb'} + p_{b'g}} \begin{pmatrix} p_{gb'} & -p_{gb'} \\ -p_{b'g} & p_{b'g} \end{pmatrix}. \quad (5)$$

In Tables V and VI we report the transition matrices in the two- and three-state HMMs for the links under analysis.

TABLE V: Transition matrices, two-state HMM

Topology2, Link 4→2	Good	Bad
Good	0.947	0.053
Bad	0.192	0.808

Topology2, Link 3→2	Good	Bad
Good	0.841	0.159
Bad	0.062	0.870

Topology1, Link 1→3	Good	Bad
Good	0.766	0.234
Bad	0.062	0.938

A. Model Implementation

To evaluate the models presented in this section, we implemented the two- and three-state HMM in the DESERT Underwater network simulation and experimentation framework [14], publicly available in [22]. The DESERT Underwater legacy physical module, called UWPhysical, computes

TABLE VI: Transition matrices, three-state HMM

Topology 2, Link 4→2	Good	Medium	Bad
Good	0.947	0.041	0.012
Medium	0.195	0.0805	0
Bad	0.179	0.071	0.750

Topology 2, Link 3→2	Good	Medium	Bad
Good	0.841	0.052	0.107
Medium	0.119	0.819	0.063
Bad	0.142	0.052	0.806

Topology 1, Link 1→3	Good	Medium	Bad
Good	0.766	0.065	0.169
Medium	0.071	0.750	0.179
Bad	0.058	0.040	0.903

the signal to noise ratio using the model presented in [1]: this model is largely used by researchers, however, it does not address the variability of the acoustic channel. For this reason, two new physical layers have been implemented in DESERT, one called UWHMMPhysical that uses the two-state HMM (Figure 3a), and one named UWHMMPhysicalExtended that uses the three-state HMM (Figure 3b). In both physical layers, the statistics of each link have been included using the so called `link-stats` objects, and the physical layer computes the probability that a packet is correctly received at a specific moment using the formula in Eq. (5) in UWH-MMPhysical, and the formula in Eq. (4) in UWHMMPhys-icalExtended, hence providing a per-link channel variability. The `link-stats` objects are independent of each other: if near nodes share the same channel, the same `link-stats` object can be used to model the channel variability in the same way. In the case of the sea experiment considered in these simulations, the links between the nodes are considered independent, hence a different `link-stats` object is used to model the channel variability between every pair of nodes.

The most relevant difference between the two- and three-state HMMs is the way the transition probabilities are computed. In the two-state HMM it is computed with the closed formula presented in Eq. (5), while for the three-state HMM the transition probability must be computed with matrix exponentiation (Eq. (4)). In order to limit the complexity of this operation for big exponents n, the exponentiation has to be performed efficiently. In our implementation we save P^n each time we compute it, so that at time step $k > n$ we can compute P^k with a number of matrix products equal to $k - n$, that is strictly less than k. As a result, the computation time of a simulation using the three-state model is not meaningfully longer than the same simulation relying on the legacy physical model or on the two-state HMM.

IV. RESULTS

A. Simulation Settings

In our simulations we analyze the system behavior with the nodes placed in the positions described in topology 1 (Figure 1a) and topology 2 (Figure 1b). The simulation lasted 18000 s in total, and we switched from topology 2 to topology

1 at time 9000 s by adding the link from node 1 to node 3 and changing the PER per link and the transition probabilities of every link accordingly. The behavior of three different communication stacks is analyzed. All stacks follow the structure presented in Figure 6: they use a constant bitrate application layer, static routing with all nodes transmitting to their 1-hop neighbors and a time division multiple access (TDMA) MAC layer. The only thing that differs in the three stacks is the physical layer: the first stack uses the legacy DESERT physical layer, the second stack uses the two-state HMM-based physical layer and, finally, the third stack employs the three-state HMM-based physical layer.
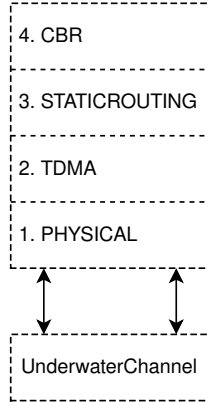
Fig. 6: Stack of the nodes in the simulations.

In the simulated network 4 nodes generate 28-bytes packets with a generation time equal to 60 s. Bandwidth and carrier frequency are set to 5 kHz and 25 kHz, respectively, in order to best simulate the behavior of the modems used in the field experiment presented in Section II. The TDMA MAC is configured with a frame duration of 8 s, equally divided between the four nodes that have a time slot of 2 s each to transmit their packets. A guard time of 0.8 s is used to avoid interference caused by the propagation time and to consider possible synchronization errors between the nodes. The simulation parameters are summarized in Table VII.

TABLE VII: Simulations parameters

| Parameter	Value
Nodes	4
Packet Size	28 Bytes
Tx Duration	18000 s
Tx Power	165 dB re 1 μPa @1 m
Frequency	25 kHz
Bandwidth	5 kHz
Bitrate	600 bps
Cbr Period	60 s
TDMA Frame	8 s
TDMA Guard Time	0.8 s

At the end of the simulations we observed the performance of each link of the network by computing PER and throughput averaged over 50 simulation runs.
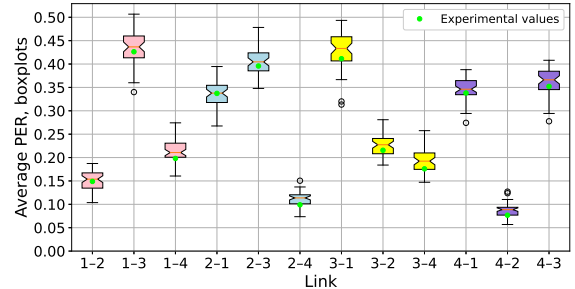
B. Simulation Results

Figure 7 presents the boxplots of the PER per link obtained with the three physical layers described in Section IV-A, and compares it with the PER measured during the sea trial (green circles). Uwphysical (Figure 7a) provides a very low PER,
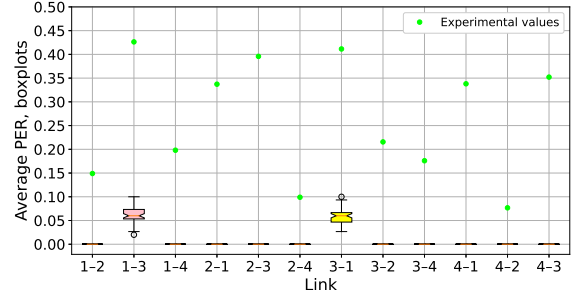
(a) PER obtained with Uwphysical.
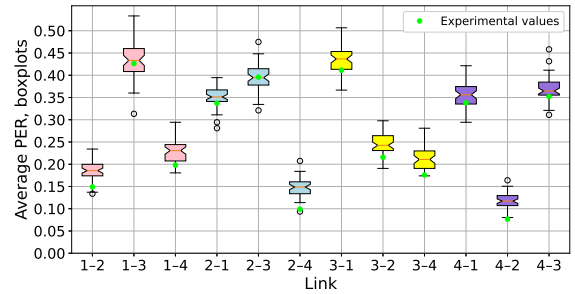
(b) PER obtained with Uwhmmphy.

(c) PER obtained with Uwhmmphyext.

Fig. 7: PER results yielded by the three simulations (boxplots) with respect to Haifa Harbor measurements (green circles).

equal to zero for all links between nodes within a distance of 1.1 km, i.e., all links except the one connecting node 1 and node 3, which are 1.2 km from each other. From a range of 1.1 km, the PER computed by this model increases up to 1 when the distance between nodes is more than 1.6 km. This implies that only the link between node 1 and node 3 has a non-zero PER, but still the real PER values are underestimated. Conversely, the PER obtained with both the two-state (Figure 7b) and the three-state (Figure 7c) models is very similar to the one observed in the sea trial, with the three-state model having a PER that matches almost perfectly the experimental one, outperforming the other two models.

5

Figure 8 presents the throughput of each link. Similarly, the throughput observed with Uwphysical (Figure 8a) is almost the same for all of the links, and is equal to 3.7 bps: only in the link between nodes 1 and 3 the throughput is approximately 1.85 bps, as that link was removed at simulation time 9000 s, when the network topology was changed from topology 1 to topology 2. With a higher PER per link, the throughput observed with the two- and three-state HMM is significantly different on different links providing results that are definitely closer to those that can be observed during a sea experiment.
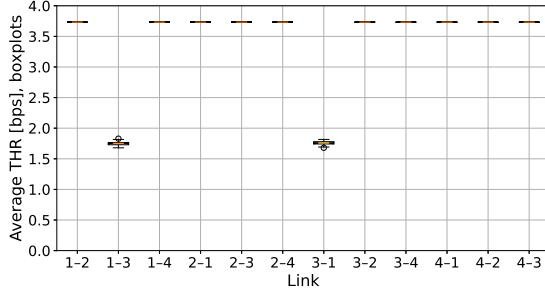
(a) Uwphysical results for THR
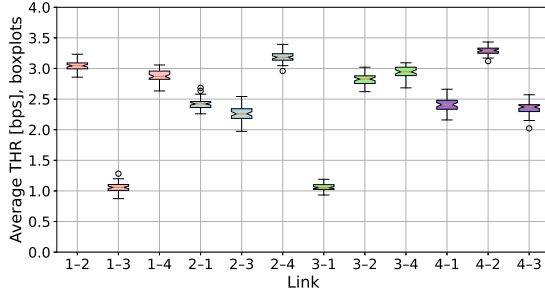
(b) Uwhmmphy results for THR
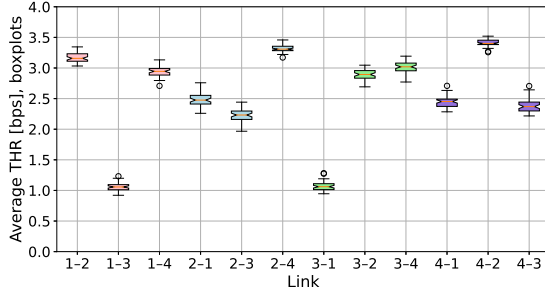
(c) Uwhmmphyext results for THR

Fig. 8: THR results yielded by the three simulations with respect to Haifa Harbor measurements.

Finally, in Figure 9 we present some plots showing the variability of throughput in time (i.e., computed every 300 seconds) for the links from node 1 to node 3 (Figure 9a), from node 3 to node 2 (Figure 9b) and from node 4 to node 2 (Figure 9c). Again, we see how optimistic the results obtained using Uwphysical are. Figure 9a highlights the throughput jump at $9000s$ for the link $1 \rightarrow 3$, due to the switch from
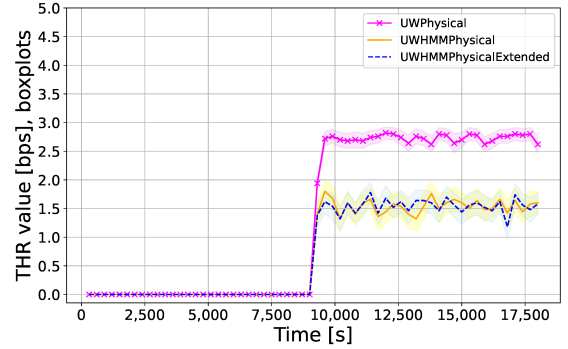
(a) Link from node 1 to node 3 inst. THR
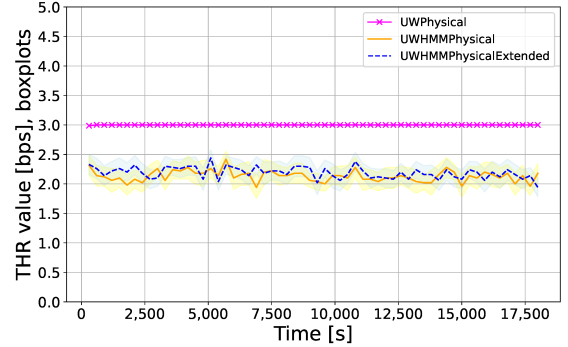
(b) Link from node 3 to node 2 inst. THR
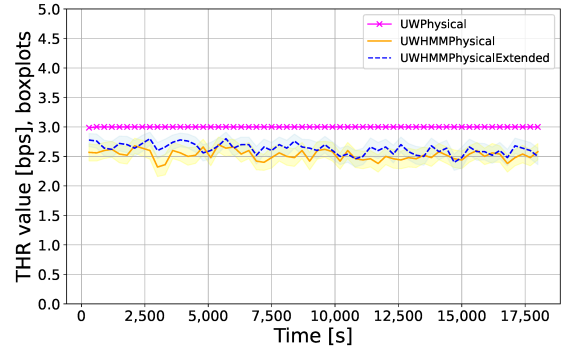
(c) Link from node 4 to node 2 inst. THR

Fig. 9: Variability of throughput in time yielded by UW-Physical, UWHMMPhysical and UWHMMPhysicalExtended modules for three relevant links

topology 2 (where the link was not in place) to topology 1. Moreover, the values for the throughput are constant for UWPhysical, except for the link $1 \leftrightarrow 3$, which is the only one having a PER greater than zero. Conversely, the estimates of the HMMs have a higher variance and are more realistic.

V. CONCLUSIONS

We were able to develop a quite precise channel model for underwater communications starting from the analysis of real field experimental data retrieved from ASUNA. The model is based on Markov chain theory and provides accurate estimates

while being not particularly computationally demanding, as well as adaptable to multiple configurations and flexible. Furthermore, it has been extensively tested in the DESERT simulator and compared with existing channel models already available, and was observed to provide accurate performance and high reliability. Possible future work may consist in investigating models with an increased number of states (i.e., more than 3), and studying the tradeoff given by the increased computational requirements and the fidelity of the results.

References

[1] M. Stojanovic, "On the relationship between capacity and distance in an underwater acoustic communication channel," *ACM SIGMOBILE Mobile Computing and Communications Review*, vol. 11, no. 4, pp. 34–43, Oct. 2007.

[2] A. Caiti, K. Grythe, J. M. Hovem, S. M. Jesus, A. Lie, A. Munafò, T. A. Reinen, A. Silva, and F. Zabel, "Linking acoustic communications and network performance: Integration and experimentation of an underwater acoustic network," *IEEE Journal of Oceanic Engineering*, vol. 38, no. 4, pp. 758–771, Sept. 2013.

[3] M. Chitre and K. Pelekanakis, "Channel variability measurements in an underwater acoustic network," in *Underwater Communications and Networking (UComms)*, Sestri Levante, Italy, 2014.

[4] M. Chitre, I. Topor, R. Bhatnagar, and V. Pallayil, "Variability in link performance of an underwater acoustic network," in *MTS/IEEE OCEANS*, Bergen, Norway, jun 2013.

[5] M. Chitre, T.-B. Koay, G. Deane, and G. Chua, "Variability in shallow water communication performance near a busy shipping lane," in *Fifth Underwater Communications and Networking Conference (UComms)*, Virtual, 2021.

[6] M. Porter *et al.*, "Bellhop code," Last time accessed: Apr. 2022. [Online]. Available: http://oalib.hlsresearch.com/Rays/index.html

[7] P. Casari, F. Campagnaro, E. Dubrovinskaya, R. Francescon, A. Dagan, S. Dahan, M. Zorzi, and R. Diamant, "ASUNA: A Topology Data Set for Underwater Network Emulation," *IEEE Journal of Oceanic Engineering*, vol. 46, no. 1, pp. 307–318, Mar. 2021.

[8] B. Tomasi, P. Casari, M. Zorzi, G. Zappa, and K. McCoy, "Experimental study of the acoustic channel properties during subnet 2009," University of Padova, Tech. Rep., 2010. [Online]. Available: {http://telecom.dei.unipd.it/pages/read/75/}

[9] B. Tomasi, J. Preisig, and M. Zorzi, "On the predictability of underwater acoustic communications performance: The KAM11 data set as a case study," in *Proc. International Conference on Underwater Networks & Systems (WUWNet)*, Seattle, WA, US, December 2011.

[10] P. A. van Walree and M. E. G. D. Colin, "In situ performance prediction of a coherent acoustic modem in a reverberant environment," *IEEE Journal of Oceanic Engineering*, vol. 47, no. 1, pp. 236–254, Jan. 2022.

[11] R. Otnes, P. A. van Walree, H. Buen, and H. Song, "Underwater acoustic network simulation with lookup tables from physical-layer replay," *IEEE Journal of Oceanic Engineering*, vol. 40, no. 4, pp. 822–840, Oct. 2015.

[12] V. Kalaiarasu, H. Vishnu, A. Mahmood, and M. Chitre, "Predicting underwater acoustic network variability using machine learning techniques," in *IEEE/MTS OCEANS*, Anchorage, US, Sept 2017.

[13] F. Campagnaro, A. Signori, R. Otnes, M. Goetz, D. Sotnik, A. Komulainen, I. Nissen, F. Favaro, F. Guerra, and M. Zorzi, "A simulation framework for smart adaptive long- and short-range acoustic networks," in *Proc. MTS/IEEE Oceans*, Virtual Global Oceans San Diego - Porto, Sept. 2021.

[14] F. Campagnaro *et al.*, "The DESERT underwater framework v2: Improved capabilities and extension tools," in *Proc. Ucomms*, Lerici, Italy, Sep. 2016.

[15] F. Pignieri, F. De Rango, F. Veltri, and S. Marano, "Markovian approach to model underwater acoustic channel: Techniques comparison," in *IEEE Military Communications Conference (MILCOM 2008)*, 2008.

[16] B. Tomasi, P. Casari, L. Finesso, G. Zappa, K. McCoy, and M. Zorzi, "On modeling JANUS packet errors over a shallow water acoustic channel using Markov and hidden Markov models," in *IEEE Military Communications Conference (MILCOM 2010)*, 2010, pp. 2406–2411.

[17] W. Turin and R. van Nobelen, "Hidden Markov modeling of flat fading channels," *IEEE Journal on Selected Areas in Communications*, vol. 16, no. 9, pp. 1809–1817, Dec. 1998.

[18] J. G. Ruiz, B. Soret, M. C. Aguayo-Torres, and J. T. Entrambasaguas, "On finite state Markov chains for Rayleigh channel modeling," in *Proc. 1st International Conference on Wireless Communication, Vehicular Technology, Information Theory and Aerospace Electronic Systems Technology*, Aalborg, Denmark, May 2009.

[19] "A shared underwater network emulation dataset," https://sites.google.com/marsci.haifa.ac.il/asuna/, Last time accessed: Apr. 2022.

[20] R. Diamant, G. N. Shirazi, and L. Lampe, "Robust spatial reuse scheduling in underwater acoustic communication networks," *IEEE Journal of Oceanic Engineering*, vol. 39, no. 1, pp. 32–46, Jan. 2014.

[21] H. M. Taylor and S. Karlin, *An Introduction to Stochastic Modeling*, 3rd ed. Academic Press, 1999.

[22] "Design, simulate, emulate and realize test-beds for underwater network protocols," http://desert-underwater.dei.unipd.it/, Last time accessed: Apr. 2022.